EARTHQUAKE ENGINEERING AND STRUCTURAL DYNAMICS
Earthquake Engng. Struct. Dyn. **28**, 1449–1467 (1999)

IDENTIFICATION OF LINEAR STRUCTURAL SYSTEMS USING EARTHQUAKE-INDUCED VIBRATION DATA

H. LUŞ[1†], R. BETTI[1*‡] AND R. W. LONGMAN[2§]

[1] *Department of Civil Engineering and Engineering Mechanics, Columbia University, New York, NY 10027, U.S.A.*
[2] *Department of Mechanical Engineering, Columbia University, New York, NY 10027, U.S.A.*

SUMMARY

This paper addresses the issue of system identification for linear structural systems using earthquake induced time histories of the structural response. The proposed methodology is based on the Eigensystem Realization Algorithm (ERA) and on the Observer/Kalman filter IDentification (OKID) approach to perform identification of structural systems using general input–output data via Markov parameters. The efficiency of the proposed technique is shown by numerical examples for the case of eight-storey building finite element models subjected to earthquake excitation and by the analysis of the data from the dynamic response of the Vincent-Thomas cable suspension bridge (Long Beach, CA) recorded during the Whittier and the Northridge earthquakes. The effects of noise in the measurements and of inadequate instrumentation are investigated. It is shown that the identified models show excellent agreement with the real systems in predicting the structural response time histories when subjected to earthquake-induced ground motion.

KEY WORDS: system identification; monitoring; linear systems; earthquake excitation

1. INTRODUCTION

For the last two decades, the problem of identifying the conditions and properties of structures by measuring their response to external excitation has been receiving considerable attention as the performances of computational algorithms and hardware have drastically increased, and various approaches have been investigated by many researchers from diverse fields of study.

In the field of identification of structures, the common practice is to create an analytical model and to update it by using static and dynamic testing.[1–3] The initial finite element model is validated by comparing the numerical eigendata (natural frequencies and mode shapes) with the eigendata acquired from the modal tests. Approaches based on frequency response functions and

* Correspondence to: R. Betti, Department of Civil Engineering and Engineering Mechanics, Columbia University, 610 Seeley W. Mudd Building, New York, NY 10027-6699, U.S.A.
† Graduate Student
‡ Associate Professor
§ Professor

Received 3 November 1998
CCC 0098–8847/99/111449–19$17·50 *Revised 27 April 1999*
 Accepted 29 June 1999

fast Fourier transforms are still dominant in the model updating philosophy partly due to tradition and to the existence of experienced personnel.[4] The aim of experimental modal analysis is to recover the system's modal characteristics, such as the natural frequencies, mode shapes, generalized masses, and loss factors, from experimental data. However, such experiments generally require a large number of actuators and sensors to pick up most of the modal data.[5] There exists a vast literature about modal analysis techniques, the details of which have been reported and discussed by Ewins,[6] while the survey by Mottershead and Friswell[5] covers a good portion of the literature on model updating methods. An alternative approach to determine an appropriate structural model is to use input–output relations to create a minimal realization that is capable of reproducing the initial input–output relations. In this context, two main frameworks, one in the time domain and one in the frequency domain, have been developed. A comparison of the complimentary papers by Beck and Jennings[7] and McVerry[8] reveals the inherent differences and identities in the two approches; in both investigations the same concept, namely that of minimizing a cost functional of the output error, is used. As studied in some later works, the frequency-domain approach seems to have the advantage of incorporating soil–structure interaction effects,[9] although these analyses are limited to very simplified soil models. On the other end, a frequency-domain approach may not be suitable for problems that require high-frequency resolution and non-linear identification,[10] where a time-domain formulation is more appropriate. Recently, time domain methodologies have become widely established, and Ghanem and Shinozuka[11,12] have reviewed some of these algorithms such as the Extended Kalman Filter (EKF)[10,13] and the recursive least squares. Şafak[14,15] reviews some adaptive techniques and identifies a SISO ARMAX model of a structure using the aftershock records of the 1985 Central Chile earthquake. Other considerable efforts, discussions and reviews on system identification of structures can be found in the works by Masri *et al.*,[16,17] Lin *et al.*,[18] Natke,[19] Udwadia,[20] Beck and Katafygiotis,[21,22] and Smyth *et al.*[23]

During the last three decades, there has been a vast number of studies and algorithms concerning the construction of state space representations in the time domain for linear dynamical systems, beginning with the works of Gilbert and Kalman.[24,25] One of the first results obtained in this field was about 'minimal realizations', indicating 'a model with the smallest state-space dimension among systems realized that has the same input–output relations within a specified degree of accuracy …'.[26] It was shown by Ho and Kalman,[27] that the minimum representation problem was equivalent to the problem of identifying the sequence of real matrices, known as the Markov parameters, which represent the unit pulse responses of a linear dynamical system. Numerous studies (i.e. References 28 and 29) have been conducted on the subject of Markov parameters and their relations to different representations of linear systems.

Following a time-domain formulation and incorporating results from control theory, Juang and Pappa[26] proposed an Eigensystem Realization Algorithm (ERA) for modal parameter identification and model reduction of linear dynamical systems, which extends the Ho–Kalman algorithm and creates a minimal realization that mimics the output history of the system when it is subjected to unit pulse inputs. Later, this algorithm was refined to better handle the effects of noise and structural non-linearities, and the ERA with data correlations (ERA/DC) was proposed.[30]

When general input data such as an earthquake-induced ground motion is used, difficulties in retrieving the system Markov parameters can arise related to problem dimensionality and numerical conditioning. Among the algorithms proposed to overcome these difficulties,[31,32] the Observer/Kalman filter IDentification (OKID) algorithm introduces an asymptotically stable

observer which increases the stability of the system and reduces the computation time, improving the performance even when noise and slight non-linearities are present. This technique has proven to be quite successful in the aerospace community in the identification of complex, high-dimensional space craft structures.

In this paper, an OKID-based approach is presented for the identification of the dynamic characteristics of multi degree-of-freedom structural systems subjected to seismic loading. The input excitation is represented by an earthquake-induced ground motion, while the output consists of the corresponding structural response. Validation of the proposed approach is presented by numerical simulations for 2-D and 3-D models of an eight-storey building (from Yang *et al.*[33]), and by the analysis of experimental data from the Vincent Thomas Bridge (Long Beach, CA). The effects of measurement noise and of the number of sensors used in the identification are discussed with examples.

2. BASIC FORMULATIONS

2.1. Input–output relations

The dynamic behaviour of an N degree of freedom linear structural system can be represented by the second-order vector differential equation

$$\mathscr{M}\ddot{\boldsymbol{\alpha}}(t) + \mathscr{C}\dot{\boldsymbol{\alpha}}(t) + \mathscr{K}\boldsymbol{\alpha}(t) = \mathscr{B}\mathbf{u}(t) \tag{1}$$

where $\boldsymbol{\alpha} \in R^N$ is the structural displacement vector in a fixed system of reference and the notation $(\dot{\ })$ indicates differentiation with respect to time. The matrices $\mathscr{M}, \mathscr{C}$, and $\mathscr{K}$, all $\in R^{N\times N}$, are the mass, damping and stiffness matrix, respectively, while $\mathscr{B} \in R^{N\times r}$ indicates the continuous time input matrix, with r denoting the dimension of the input vector $\mathbf{u}(t)$.

When the input is represented by a seismic excitation, the components of $\alpha(t)$ correspond to nodal displacements with respect to a system of reference whose origin is at the base of the structure and moves together with the base. The external forcing term $\mathscr{B}\mathbf{u}(t)$ can now be replaced by $-\mathscr{M}\mathbf{I}_{N\times 1}\ddot{x}_g(t)$, with $\mathbf{I}_{N\times 1}$ being the unitary vector and $\ddot{x}_g(t)$ the ground acceleration at time t. In this study, no soil–structure interaction has been considered. Although these effects are important on the overall structural response, a clear understanding of such a complex phenomenon is limited to the frequency domain and only to simplified soil models (e.g. homogeneous isotropic half-space, horizontal layers, etc.). For a frequency-domain approach, it is possible to obtain frequency-dependent foundation compliances that can be used for determining the transfer functions for the various input–output pairs. In time-domain formulations of soil–structure interaction, there is not a general framework to work with and the various proposed methodologies (FEM with absorbing boundaries, infinite elements, and so on) have all shown limitations, i.e. only valid for 1-D wave propagation problems and/or for a particular type of incident wave. In addition, in most real-world applications (as for the case considered in this study of the monitoring system of the Vincent–Thomas bridge), sensors are placed only on the structure (on the foundations and on the superstructure), so that the effects of the dynamic interaction between the foundation and the surrounding soil have been bypassed. It is for these reasons that, although recognizing their importance and the need for further research in this area, the soil–structure interaction effects have not been included in this study.

The same structural system of equation (1) can also be represented as a first-order vector differential equation in state-space form as

$$\dot{\mathbf{x}}(t) = \mathbf{A}\mathbf{x}(t) + \mathbf{B}\mathbf{u}(t) \tag{2}$$

$$\mathbf{y}(t) = \mathbf{C}\mathbf{x}(t) + \mathbf{D}\mathbf{u}(t) \tag{3}$$

where $\mathbf{x} = (x_1, x_2, \ldots, x_n)^{\mathrm{T}}$ is the n-dimensional state vector ($n = 2N$), and $\mathbf{y} \in R^m$ is the m-dimensional output vector. The matrices $\mathbf{A} \in R^{n \times n}$, $\mathbf{B} \in R^{n \times r}$, $\mathbf{C} \in R^{m \times n}$, and $\mathbf{D} \in R^{m \times r}$ represent the time invariant system matrices. Since we receive measurements of the input and output generated by an earthquake excitation as sets of discrete data, it is convenient to work in discrete time domain so that equations (2) and (3) can be expressed as difference equations in the following forms:

$$\mathbf{x}(k+1) = \mathbf{\Phi}\mathbf{x}(k) + \mathbf{\Gamma}\mathbf{u}(k) \tag{4}$$

$$\mathbf{y}(k) = \mathbf{C}\mathbf{x}(k) + \mathbf{D}\mathbf{u}(k) \tag{5}$$

where the integer k denotes the time-step number, i.e. $\mathbf{x}(k+1) = \mathbf{x}(k(\Delta T) + \Delta T)$ with ΔT being the time step interval. The error introduced by the discretization may be made negligible by using a time step sufficiently small compared with the significant time constant of the system. Since the sampling rate of the earthquake excitation records is usually 0·01 sec (corresponding to a cutoff frequency of 100 Hz), and civil structures have natural frequencies far below 100 Hz, the zero-order hold sampling assumption can be successfully used. For a zero-order hold approximation and a sampling time ΔT, the discrete time system matrices $\mathbf{\Phi}$ and $\mathbf{\Gamma}$ can be evaluated as $\mathbf{\Phi} = \mathrm{e}^{\mathbf{A}(\Delta T)}$ and $\mathbf{\Gamma} = (\int_0^{\Delta T} \mathrm{e}^{\mathbf{A}\sigma}\, \mathrm{d}\sigma)\mathbf{B}$, and the solution of equations (4) and (5) is given by the following convolution sum (for $k \geqslant 1$):

$$\mathbf{x}(k) = \mathbf{\Phi}^k \mathbf{x}(0) + \sum_{j=0}^{k-1} \mathbf{\Phi}^{(k-1-j)} \mathbf{\Gamma}\mathbf{u}(j) \tag{6}$$

$$\mathbf{y}(k) = \mathbf{C}\mathbf{\Phi}^k \mathbf{x}(0) + \sum_{j=0}^{k-1} \mathbf{C}\mathbf{\Phi}^{(k-1-j)} \mathbf{\Gamma}\mathbf{u}(j) + \mathbf{D}\mathbf{u}(k) \tag{7}$$

For zero initial conditions, as in earthquake related analyses, equation (7) can also be written in matrix form for a sequence of 'l' consecutive time steps as

$$\hat{\mathbf{y}}_{m \times l} = \mathbf{M}_{m \times rl} \mathbf{U}_{rl \times l} \tag{8}$$

where

$$\hat{\mathbf{y}} = [\mathbf{y}(0), \mathbf{y}(1), \mathbf{y}(2), \ldots, \mathbf{y}(l-1)] \tag{9}$$

$$\mathbf{M} = [\mathbf{D}, \mathbf{C}\mathbf{\Gamma}, \mathbf{C}\mathbf{\Phi}\mathbf{\Gamma}, \ldots, \mathbf{C}\mathbf{\Phi}^{l-2}\mathbf{\Gamma}] \tag{10}$$

and

$$\mathbf{U} = \begin{bmatrix} \mathbf{u}(0) & \mathbf{u}(1) & \mathbf{u}(2) & \cdots & \mathbf{u}(l-1) \\ & \mathbf{u}(0) & \mathbf{u}(1) & \cdots & \mathbf{u}(l-2) \\ & & \ddots & & \vdots \\ & & & \mathbf{u}(0) & \mathbf{u}(1) \\ & & & & \mathbf{u}(0) \end{bmatrix} \tag{11}$$

The matrix $\hat{\mathbf{y}}$, of dimensions $m \times l$, is a matrix whose columns are the output vectors for the l time steps, while the matrix $\mathbf{U}$ contains the input vectors for different time steps arranged in an upper-triangular form. The matrix $\mathbf{M}$ contains the parameters known as the Markov parameters.[29] These parameters are the response of the system to a unit pulse as it can be seen for the case of a single input by putting $\mathbf{u} = [1\ 0\ \cdots\ 0]$ in equation (11), leading to $\hat{\mathbf{y}} = \mathbf{M}$ in equation (8).

2.2. ERA and ERA/DC

To present, in a concise form, the fundamental theoretical principles of ERA and ERA/DC, let us consider that r impulse tests have been performed on a system with m outputs; i.e. $\mathbf{y}(k) = [y_1(k)\ y_2(k) \cdots y_m(k)]^{\mathrm{T}}$, and $\mathbf{u}(k) = [u_1(k)\ u_2(k)\ \cdots\ u_r(k)]^{\mathrm{T}}$. Let us denote with $\mathbf{y}^j(k)$ a new vector, of dimension m, which represents the system's response at time $k(\Delta T)$ to the unit impulse input $\mathbf{u}_j$ at time zero. In this way, we can package the data as

$$\mathbf{Y}(k) = [\mathbf{y}^1(k)\ \mathbf{y}^2(k)\ \cdots\ \mathbf{y}^r(k)], \quad k = 1, 2, \ldots \tag{12}$$

and form the $ms \times rs$ Hankel data matrix

$$\mathbf{H}^s(k-1) = \begin{bmatrix} \mathbf{Y}(k) & \mathbf{Y}(k+1) & \cdots & \mathbf{Y}(k+s-1) \\ \mathbf{Y}(k+1) & \mathbf{Y}(k+2) & \cdots & \mathbf{Y}(k+s) \\ \vdots & \vdots & \ddots & \vdots \\ \mathbf{Y}(k+s-1) & \mathbf{Y}(k+s) & \cdots & \mathbf{Y}(k+2(s-1)) \end{bmatrix} \tag{13}$$

where s is an integer that determines the size of such a matrix. The first Markov parameter, i.e. $\mathbf{D}$, can be readily identified by considering that

$$\mathbf{D} = \mathbf{Y}(0) \tag{14}$$

Having identified the $\mathbf{D}$ matrix, we now look for the triplet $(\mathbf{C}, \mathbf{\Phi}, \mathbf{\Gamma})$ that will reproduce the data sequence $\mathbf{Y}(k)$, $k = 1, 2, \ldots$. If the data permits a realization, then the full data sequence can be generated from the triplet $(\mathbf{C}, \mathbf{\Phi}, \mathbf{\Gamma})$ via the following equation:

$$\mathbf{Y}(k) = \mathbf{C}\mathbf{\Phi}^{k-1}\mathbf{\Gamma}, \quad k = 1, 2, 3, \ldots \tag{15}$$

Substituting equations (15) into (13) leads to the following representation of the Hankel matrix:

$$\mathbf{H}^s(i) = \begin{bmatrix} \mathbf{C}\mathbf{\Phi}^i\mathbf{\Gamma} & \mathbf{C}\mathbf{\Phi}^{i+1}\mathbf{\Gamma} & \cdots & \mathbf{C}\mathbf{\Phi}^{i+s-1}\mathbf{\Gamma} \\ \mathbf{C}\mathbf{\Phi}^{i+1}\mathbf{\Gamma} & \mathbf{C}\mathbf{\Phi}^{i+2}\mathbf{\Gamma} & \cdots & \mathbf{C}\mathbf{\Phi}^{i+s}\mathbf{\Gamma} \\ \vdots & \vdots & \ddots & \vdots \\ \mathbf{C}\mathbf{\Phi}^{i+s-1}\mathbf{\Gamma} & \mathbf{C}\mathbf{\Phi}^{i+s}\mathbf{\Gamma} & \cdots & \mathbf{C}\mathbf{\Phi}^{i+2(s-1)}\mathbf{\Gamma} \end{bmatrix}, \quad i = 0, 1, \ldots \tag{16}$$

which presents the following properties:

(1) If there exists a finite-dimensional realization $(\mathbf{C}, \mathbf{\Phi}, \mathbf{\Gamma})$ of the data sequence $\mathbf{Y}(k)$, $k = 1, 2, 3, \ldots$, and if the dimension of a minimal realization is n, then

$$\text{rank } \mathbf{H}^s(i) = n, \quad \forall s \geqslant n, \quad \text{and } i = 0, 1, 2, \ldots \tag{17}$$

(2) If the data sequence is to have a finite-dimensional realization, then there must exist a finite integer n and scalar values β_k such that

$$\mathbf{Y}(n+1+j) = -\sum_{k=1}^{n} \beta_k \, \mathbf{Y}(j+k) \quad \text{for } j = 0, 1, 2, \ldots \tag{18}$$

Once the system's Markov parameters have been determined and the corresponding Hankel matrix has been built, let the singular value decomposition of $\mathbf{H}^s(0)$ be denoted by

$$\mathbf{H}^s(0) = \mathbf{U}\Sigma\mathbf{V}^{\mathrm{T}} = [\mathbf{U}_1 \;\; \mathbf{U}_2] \begin{bmatrix} \mathbf{S} & \mathbf{0} \\ \mathbf{0} & \mathbf{0} \end{bmatrix} \begin{bmatrix} \mathbf{V}_1^{\mathrm{T}} \\ \mathbf{V}_2^{\mathrm{T}} \end{bmatrix} = \mathbf{U}_1 \mathbf{S} \mathbf{V}_1^{\mathrm{T}} \tag{19}$$

where $\mathbf{U}_{ms \times ms}$ and $\mathbf{V}_{rs \times rs}$ are unitary matrices, and $\mathbf{S}$ is a square diagonal matrix (the non-zero partition of $\mathbf{\Sigma}_{ms \times rs}$) whose dimensions equal to the rank of the $\mathbf{H}^s(0)$ matrix. The basic theorem of the ERA realization states that, if the dimension of any minimal realization is n, then the following triplet is a minimal realization for any $s \geqslant n$:

$$\mathbf{\Phi} = \mathbf{S}^{-1/2} \mathbf{U}_1^{\mathrm{T}} \mathbf{H}^s(1) \, \mathbf{V}_1 \mathbf{S}^{-1/2} \tag{20}$$

$$\mathbf{\Gamma} = \mathbf{S}^{1/2} \mathbf{V}_1^{\mathrm{T}} \mathbf{E}_r \tag{21}$$

$$\mathbf{C} = \mathbf{E}_m^{\mathrm{T}} \mathbf{U}_1 \mathbf{S}^{1/2} \tag{22}$$

where $\mathbf{E}_r$ is $[\mathbf{I}_{r \times r} \;\; 0 \;\; 0 \;\; \cdots \;\; 0]^{\mathrm{T}}_{r \times rs}$, and $\mathbf{E}_m$ is defined analogously. Hence, the initially unknown matrices $\mathbf{\Phi}$, $\mathbf{\Gamma}$, $\mathbf{C}$ and $\mathbf{D}$, can be obtained using the ERA formulation once the system's Markov parameters have been identified. By converting the realized discrete time system matrix $\mathbf{\Phi}$ to the continuous time equivalent one, $\mathbf{A}$, and considering its eigenvalues, it is then possible to extract the modal frequencies and damping factors of the identified structural system. Furthermore, it is also possible to extract the information on second-order mode shapes, modal participation factors, and the 'true' damping matrix without any assumption of diagonal modal damping following the procedure presented in References 34 and 35.

It is important to notice that the ERA algorithm does not necessarily use the Hankel matrix. Instead, making use of the supposed linear dependence within the Hankel matrix, it constructs a generalized Hankel matrix,

$$\mathbf{H}^{ls}(k-1) = \begin{bmatrix} \mathbf{Y}(k) & \mathbf{Y}(k+1) & \cdots & \mathbf{Y}(k+s-1) \\ \mathbf{Y}(k+1) & \mathbf{Y}(k+2) & \cdots & \mathbf{Y}(k+s) \\ \vdots & \vdots & \ddots & \vdots \\ \mathbf{Y}(k+l-1) & \mathbf{Y}(k+l) & \cdots & \mathbf{Y}(k+l+s-2) \end{bmatrix} \tag{23}$$

which amounts to deleting some row partitions of the Hankel matrix. Increasing the amount of data used in the identification decreases the variance of the identified parameters, but conversely increases the bias in the estimated parameters. This is because noise and numerical errors show up most readily in the singular values of the generalized Hankel matrix. For an ideal case, if the minimal realization of a system has the dimension n, then the rank of the $\mathbf{H}^{ls}(0)$ matrix should be n, and all the other singular values should be zero. However, in the presence of noise, some structural non-linearities, and numerical errors, these singular values are not zero, and sometimes

there can be difficulties in deciding what can be effectively considered as zero. To overcome this problem, Juang and Pappa[26] develop two indicators, (i) the modal amplitude coherence and (ii) the modal phase collinearity, which, together with the singular values of the $\mathbf{H}^{ls}(0)$ matrix, form a basis for a rational choice of the model size.

In order to reduce the bias due to noise in the data, an alternative formulation of the ERA can be used.[30] Such an identification algorithm, called the ERA/DC, combines the minimum order realization approach with insights from the Correlation Fit method, using auto correlations and cross-correlations of output data instead of actual response data.

It should also be noted that a system has an infinite number of minimal realizations, since, given a minimal realization $(\mathbf{C}, \mathbf{\Phi}, \mathbf{\Gamma})$ and for any non-singular transformation matrix $\mathscr{T}$, the triplet $(\mathscr{T}\mathbf{\Phi}\mathscr{T}^{-1}, \mathscr{T}\mathbf{\Gamma}, \mathbf{C}\mathscr{T}^{-1})$ is also a minimal realization and the eigenvalues of $\mathbf{\Phi}$ are unchanged. Therefore, it is meaningless to compare any two minimal realizations of a system unless both are transformed to a common reference.

2.3. *Observer/Kalman filter IDentification*

Having established a basis for the realization theory, let us address the question on how to extract the Markov parameters when general input–output data are given. One approach is to use the fast Fourier transforms, and obtain the pulse responses, which has some drawbacks such as (i) the need for a sufficiently rich input and (ii) the transformation of the problem to the frequency domain. In a time-domain formulation, the approach is to solve for the Markov parameters directly from the input–output data. This approach seems attractive, especially for single input systems as in the case of structures subjected to an earthquake excitation, where the input matrix $\mathbf{U}$ in equation (11) becomes a square matrix.

For an asymptoptically stable system, let p be a sufficiently large integer such that $\mathbf{\Phi}^h \approx \mathbf{C}\mathbf{\Phi}^h\mathbf{\Gamma} \approx 0$ for any $h \geqslant p$. Then equation (8) can be approximated as

$$\hat{\mathbf{y}}_{m\times l} \approx \mathbf{M}_{m\times r(p+1)}\mathbf{U}_{r(p+1)\times l} \tag{24}$$

where

$$\hat{\mathbf{y}} = [\mathbf{y}(0)\ \ \mathbf{y}(1)\ \ \mathbf{y}(2)\ \ \cdots\ \ \mathbf{y}(p)\ \ \cdots\ \ \mathbf{y}(l-1)] \tag{25}$$

$$\mathbf{M} = [\mathbf{D}\ \ \mathbf{C}\mathbf{\Gamma}\ \ \mathbf{C}\mathbf{\Phi}\mathbf{\Gamma}\ \ \cdots\ \ \mathbf{C}\mathbf{\Phi}^{p-1}\mathbf{\Gamma}] \tag{26}$$

and

$$\mathbf{U} = \begin{bmatrix} \mathbf{u}(0) & \mathbf{u}(1) & \mathbf{u}(2) & \cdots & \mathbf{u}(p) & \cdots & \mathbf{u}(l-1) \\ & \mathbf{u}(0) & \mathbf{u}(1) & \cdots & \mathbf{u}(p-1) & \cdots & \mathbf{u}(l-2) \\ & & \mathbf{u}(0) & \cdots & \mathbf{u}(p-2) & \cdots & \mathbf{u}(l-3) \\ & & & \ddots & \vdots & \cdots & \vdots \\ & & & & \mathbf{u}(0) & \cdots & \mathbf{u}(l-p-1) \end{bmatrix} \tag{27}$$

The matrices $\mathbf{M}$ and $\mathbf{U}$ have been truncated according to the value of p. If the data is to have a realization, then the Markov parameters approximately satisfy the equation $\mathbf{M} = \mathbf{y}\mathbf{U}^{\dagger}$ where $\mathbf{U}^{\dagger}$ is the pseudo inverse of the input matrix $\mathbf{U}$, and the error due to such an approximation decreases as p increases. However, for lightly damped structures the integer p, and therefore the

size of **U** is practically too large to perform the inversion operation numerically. In order to overcome such a limitation, the system input–output relations can be described by a new set of state space equations which are obtained by adding and subtracting the term $\mathbf{R}\mathbf{y}(k)$ in equation (4) as presented in Reference 32. This will lead to:

$$\begin{aligned}\mathbf{x}(k+1) &= \mathbf{\Phi}\mathbf{x}(k) + \mathbf{\Gamma}\mathbf{u}(k) + \mathbf{R}\mathbf{y}(k) - \mathbf{R}\mathbf{y}(k)\\ &= (\mathbf{\Phi} + \mathbf{RC})\mathbf{x}(k) + (\mathbf{\Gamma} + \mathbf{RD})\mathbf{u}(k) - \mathbf{R}\mathbf{y}(k)\\ &= \bar{\mathbf{\Phi}}\mathbf{x}(k) + \bar{\mathbf{\Gamma}}\boldsymbol{v}(k) \qquad (28)\\ \mathbf{y}(k) &= \mathbf{C}\mathbf{x}(k) + \mathbf{D}\mathbf{u}(k) \qquad (29)\end{aligned}$$

where

$$\bar{\mathbf{\Phi}} = (\mathbf{\Phi} + \mathbf{RC}) \qquad (30)$$

$$\bar{\mathbf{\Gamma}} = [(\mathbf{\Gamma} + \mathbf{RD})(-\mathbf{R})] \qquad (31)$$

$$\boldsymbol{v}(k) = \begin{bmatrix}\mathbf{u}(k)\\ \mathbf{y}(k)\end{bmatrix} \qquad (32)$$

The gain matrix **R** is chosen to make the system represented by equations (28) and (29) as stable as desired. Although equations (4) and (28) are mathematically identical, equation (28) can be considered as an observer equation and the Markov parameters of this new system, denoted as $\bar{\mathbf{M}}$, are called the observer's Markov parameters. If the matrix **R** is chosen in such a way that $\bar{\mathbf{\Phi}}$ is asymptotically stable, then $\mathbf{C}\bar{\mathbf{\Phi}}^{h}\bar{\mathbf{\Gamma}} \approx \mathbf{0}$ for $h \geqslant p$, and we can solve for $\bar{\mathbf{M}}$ from real input–output data using

$$\hat{\mathbf{y}}_{m\times l} \approx \bar{\mathbf{M}}_{m\times((r+m)p+r)}\mathbf{V}_{((r+m)p+r)\times l} \qquad (33)$$

$$\bar{\mathbf{M}} = \hat{\mathbf{y}}\mathbf{V}^{\dagger} \qquad (34)$$

where

$$\hat{\mathbf{y}} = [\mathbf{y}(0)\ \ \mathbf{y}(1)\ \ \mathbf{y}(2)\ \ \cdots\ \ \mathbf{y}(p)\ \ \cdots\ \ \mathbf{y}(l-1)] \qquad (35)$$

$$\bar{\mathbf{M}} = [\mathbf{D}\ \ \mathbf{C}\bar{\mathbf{\Gamma}}\ \ \mathbf{C}\bar{\mathbf{\Phi}}\bar{\mathbf{\Gamma}}\ \ \cdots\ \ \mathbf{C}\bar{\mathbf{\Phi}}^{p-1}\bar{\mathbf{\Gamma}}] \qquad (36)$$

and

$$\mathbf{V} = \begin{bmatrix}\mathbf{u}(0) & \mathbf{u}(1) & \mathbf{u}(2) & \cdots & \mathbf{u}(p) & \cdots & \mathbf{u}(l-1)\\ & \boldsymbol{v}(0) & \boldsymbol{v}(1) & \cdots & \boldsymbol{v}(p-1) & \cdots & \boldsymbol{v}(l-2)\\ & & \boldsymbol{v}(0) & \cdots & \boldsymbol{v}(p-2) & \cdots & \boldsymbol{v}(l-3)\\ & & & \ddots & \vdots & \cdots & \vdots\\ & & & & \boldsymbol{v}(0) & \cdots & \boldsymbol{v}(l-p-1)\end{bmatrix} \qquad (37)$$

If p is large enough, it can be shown[32] that the identified observer Markov parameters will converge to those of an optimal Kalman filter, justifying the name of Observer/Kalman filter IDentification.

Having identified the observer Markov parameters, the true system's Markov parameters can be retrieved using the recursive formula:

$$\mathbf{M}_k = \bar{\mathbf{M}}_k^{(1)} + \sum_{i=0}^{k-1}\bar{\mathbf{M}}_i^{(2)}\mathbf{M}_{k-i-1} + \bar{\mathbf{M}}_k^{(2)}\mathbf{D} \qquad (38)$$

where

$$\bar{\mathbf{M}} = [\bar{\mathbf{M}}_{-1} \;\; \bar{\mathbf{M}}_0 \;\; \bar{\mathbf{M}}_1 \;\; \cdots \;\; \bar{\mathbf{M}}_{p-1}] \tag{39}$$

$$\begin{aligned} \bar{\mathbf{M}}_k &= \mathbf{C}\bar{\mathbf{\Phi}}^k \bar{\mathbf{\Gamma}} \\ &= [\mathbf{C}(\mathbf{\Phi} + \mathbf{RC})^k(\mathbf{\Gamma} + \mathbf{RD}), \quad -\mathbf{C}(\mathbf{\Phi} + \mathbf{RC})^k \mathbf{R}] \\ &= [\bar{\mathbf{M}}_k^{(1)}, \quad \bar{\mathbf{M}}_k^{(2)}], \quad k = 1, 2, 3, \ldots \end{aligned} \tag{40}$$

with $\bar{\mathbf{M}}_{-1} = \mathbf{D}$. The reader should refer to the work of Juang *et al.*[32] for details concerning the direct identification of the observer gain $\mathbf{R}$ and the relation between the identified observer and a Kalman filter.

Once the system's Markov parameters have been identified, they can be used in the previous ERA formulation for the identification of the dynamic structural characteristics.

3. NUMERICAL RESULTS

3.1. Two-dimensional eight-storey shear building

In order to validate the proposed approach for the case of seismic excitation of structural systems, let us first consider a discrete mass — dashpot — spring model of an eight-storey building, with a floor mass of 345·6 tons and floor stiffness equal to 340 400 kN/m.[33] The damping matrix is set up so to penalize the identification of higher modes with 2 per cent modal damping for the first four modes, and 5 per cent modal damping for the higher modes. The natural frequencies of such a system (5·79, 17·18, 27·98, 37·83, 46·39, 53·37, 58·53, and 61·7 rad/sec) will be used as benchmark for comparing the various identification attempts. The input–output data to be used in the identification algorithm is obtained through numerical simulations using the Northridge 94 9 earthquake ground acceleration record as the input excitation, while the output measurements are the simulated floor accelerations. We should mention that this set of ground accelerations does not excite the higher modes of the structure very well (actually quite poorly for the highest two modes), and that this would be a problem for the more conventional identification techniques. The noise is simulated by adding a normally distributed disturbance (with zero mean and 0·001 m/sec/sec standard deviation) to the output, inducing high relative errors when the output is not large in magnitude.

The identified modal frequencies and damping factors are presented in Tables I and II, varying the number and the location of sensors used in the identification. When there is no noise in the measurements, the system can be identified (for all the numbers of sensors investigated) with perfect accuracy for any p such that $mp \geqslant n$. However, when there is noise present in the measurements, one needs to have a value for p large enough so that more data points are employed, leading to a better identification of modal characteristics (one should identify a higher-order system, and then reduce the size by modal reduction, e.g. by comparing the pulse responses of the initial and reduced models). For comparative purposes, we have identified various systems using different values of p, and then reduced them to 16th order systems; this choice of the system order is justified by looking at the singular value plots of the initial models. The lower-order modes, which are well excited by the input excitation, can be identified 'almost exactly', and they converge very quickly. Even with only two sensors, the first six frequencies and their associated

Table I. Identified modal frequencies (rad/sec) with various number of sensors for the eight-storey shear building, with and without noise

Actual	Identified					
	2 sensors	8 sensors	4 sensors	2 sensors with noise		
	No noise	Noise	Noise	1 and 8	4 and 5	4 and 8
5·791	5·791	5·791	5·791	5·792	5·792	5·791
17·177	17·177	17·177	17·177	17·177	17·177	17·177
27·978	27·978	27·978	27·978	27·978	27·977	27·978
37·826	37·826	37·826	37·826	37·826	37·829	37·826
46·386	46·386	46·386	46·385	46·369	46·489	46·318
53·366	53·366	53·377	53·300	53·571	53·206	53·534
58·529	58·529	58·566	58·732	58·730	60·732	61·188
61·699	61·699	61·757	62·086	170·374	316·978	308·941

Table II. Identified modal damping percentages (%) with various number of sensors for the 8-storey shear building, with and without noise

Actual	Identified					
	2 sensors	8 sensors	4 sensors	2 sensors with noise		
	No noise	Noise	Noise	1 and 8	4 and 5	4 and 8
2·0	2·0	2·0	2·0	2·0	2·0	2·0
2·0	2·0	2·0	2·0	2·0	2·0	2·0
2·0	2·0	2·0	2·0	2·0	2·0	2·0
2·0	2·0	2·0	2·0	2·0	2·0	2·0
5·0	5·0	5·0	5·0	4·9	4·7	5·2
5·0	5·0	5·0	5·0	5·0	4·8	4·7
5·0	5·0	5·1	5·5	5·8	4·2	5·6
5·0	5.0	5·3	5·5	3·9	13·3	1·2

modal damping values are identified quite successfully. It can be observed that the location of the sensors affects the success of the identification when the instrumentation is not adequate. For the higher modes that are not well excited, the convergence requires more data points, and the values are only approximate. Figures 1 and 2 show how the identified highest natural frequency and the corresponding modal damping percentage converge as more data is used.

We should also mention that when only one sensor is used, the modal characteristics can not be exactly identified even when there is no noise present, although the relative error in frequencies for the first six modes is almost zero. To identify the higher frequencies, more sensors are required.

3.2. Three-dimensional eight-storey building

To test the effectiveness of the proposed identification approach on a more 'realistic' case, three dimensional models of an eight-storey building with rigid floors, of base dimensions 20×10 m

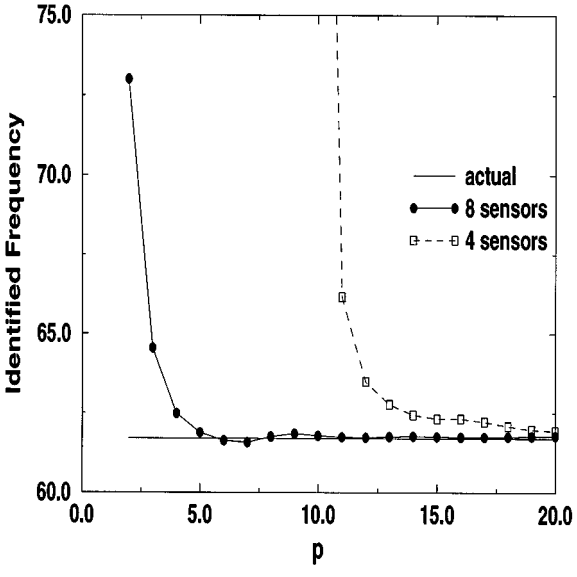

Figure 1. Identified values of the highest frequency (rad/sec) for various values of p

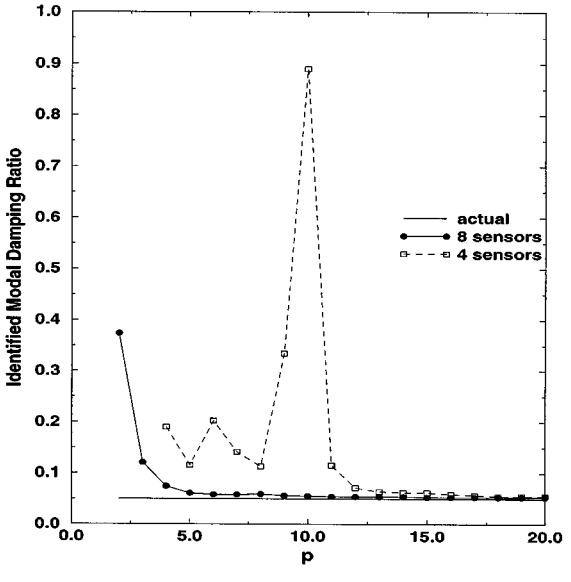

Figure 2. Identified values of the modal damping ratio associated with the highest frequency for various values of p

have been considered, using the previous 2-D model as a base. The building has three equally spaced frames along the major axis and two along the minor axis, with a translational floor stiffness of $K_{\max} = 340\,400$ kN/m along the major direction and of $K_{\min} = 255\,300$ kN/m in the minor direction ($K_{\min} = 3/4K_{\max}$). In order to excite torsional modes, the model is made slightly

Table III. Identified modal frequencies (ω, rad/sec) and modal damping percentages (ζ,%) with various floor accelerations (three per floor) for the 3-D structure with noise included

ω (rad/sec)					ζ (%)				
Actual	Identified				Actual	Identified			
	Sensor location					Sensor location			
	All floors	1,3,5,8	1,8	8		All floors	1,3,5,8	1,8	8
8·38	8·38	8·38	8·38	8·38	2	2	2	2	2
10·48	10·48	10·48	10·48	10·48	2	2	2	2	2
15·22	15·22	15·22	15·22	15·22	2	2	2	2	2
24·85	24·85	24·85	24·85	24·85	2	2	2	2	2
31·07	31·07	31·07	31·07	31·07	5	5	5	5	5
40·48	40·48	40·48	40·47	40·43	5	5	5	5	5
45·13	45·14	45·14	45·13	45·14	5	5	5	5	5
50·61	50·61	50·61	50·61	50·61	5	5	5	5	5
54·72	54·72	54·72	54·72	54·68	5	5	5	5	5
67·11	67·13	67·13	67·14	67·54	5	5	5	5	4
68·42	68·42	68·41	68·42	68·40	5	5	5	5	5
73·51	73·60	73·71	73·78	73·66	5	5	5	5	5
77·21	77·32	77·21	77·30	81·92	5	5	5	6	5
83·90	83·91	83·91	83·96	84·07	5	5	5	5	5
84·68	84·74	85·07	85·46	148·14	5	5	6	6	1

irregular by increasing the stiffness of the two columns of the first frame with respect to the other columns on each floor. The earthquake excitation is represented by recorded time histories of the ground acceleration from the 1994 Northridge earthquake (stations USC0020 and USC0021) applied along two orthogonal directions. The relative accelerations of the structural joints were obtained through a modal superposition analysis using the first 15 modes of the structure. In this analysis it is assumed that there are three accelerometers on each floor, with two in major direction and one in minor direction for the odd numbered floors, and two in the minor direction and one in the major direction for the even numbered floors. Table III clearly shows that all structural modes can be successfully identified with adequate instrumentation even when noise is present. If only the output measurements of the eighth floor are used, most vibrational modes can be picked up with high accuracy, although the highest modes need more information for a successful identification.

3.3. Vincent–Thomas bridge

The Vincent–Thomas suspension bridge, constructed in the early 1960s, is located in Los Angeles Harbor. The bridge superstructure has a centre span of 1500 ft, and two side spans of

Table IV. Vertically dominant modal frequencies (ω, Hz) and modal damping percentages (ζ, %) as reported by Niazy[36] and as identified by OKID using only vertical outputs

Niazy						OKID			
Calculated (FEM model)		Ambient vibrations		Whittier earthquake		Whittier earthquake		Northridge earthquake	
ω	ζ, %	ω	ζ, %	ω	ζ, %	ω	ζ, %	ω	ζ, %
0·201	6·0	0·216	1·6	0·209	4·8	0·234	1·53	0·225	1·72
0·223	3·0	0·234	2·3	0·224	4·8	0·388	38·18	0·304	28·64
0·336	1·0	0·366	0·6	0·363	5·8	0·464	9·69	0·459	1·76
0·344	3·5	—	—	0·373	5·4	0·576	9·88	0·533	4·03
0·422	5·0	0·487	0·9	0·448	7·1	0·6170	14·50	0·600	26·20
0·526	3·5	0·579	0·5	0·562	5·4	0·6174	76·77	0·632	13·73
0·772	3·0	0·835	5·6	0·806	0·8	0·769	29·69	0·791	15·58
1·065	0·1	1·121	0·4	—	—	0·804	1·44	0·811	0·97
1·082	0·1	1·022	0·5	—	—	0·857	11·60	0·974	2·69
1·083	0·1	1·077	0·4	—	—	0·947	4·32	1·110	0·60

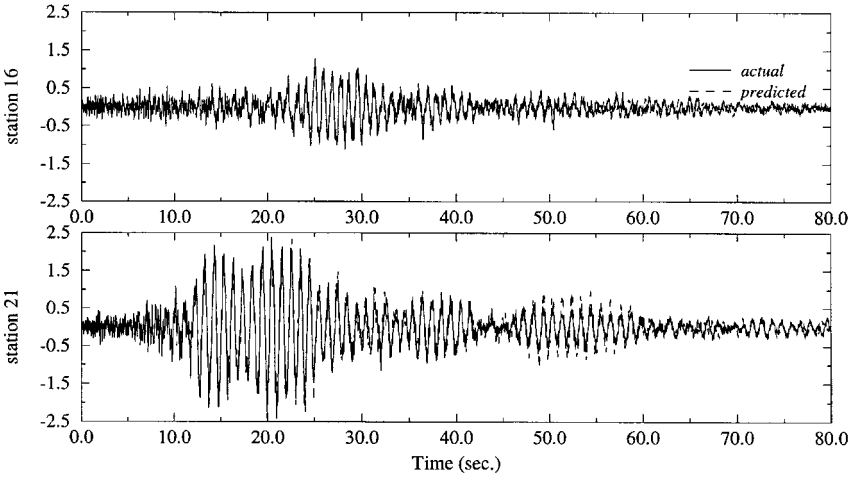

Figure 3. Actual and predicted accelerations (m/sec/sec) for the Vincent–Thomas Bridge during the Whittier earthquake

506·5 ft. The strong-motion intrumentation is installed and maintained by the California Division of Mines and Geology; there are 26 sensors located on the superstructure and on the supports. Many reported studies about the dynamic properties of the bridge exist; here we will refer to the extensive study by Niazy.[36] In the present analysis, the data obtained during the 1987 Whittier earthquake and the 1994 Northridge earthquake have been used for the identification of structural parameters. It is known that the response was highly non-linear during the peak times of the Northridge earthquake; therefore, for identification purposes we will use the final 50 sec of

the records, in which the strong ground accelerations have died out. In this study, the inputs are the 10 acceleration records from sensors located at the base of the structure, and the outputs are the vertical accelerations of the superstructure, with four sensors belonging to the center span and one sensor on one of the sidespans. In Table IV, the lowest vertical frequencies and the corresponding modal damping percentages as reported by Niazy, and as identified in this study, are presented. Figure 3 shows the actual and predicted responses of two of the output channels used in the analysis of the Whittier earthquake, and Figure 4 shows the actual and predicted responses of three of the channels used in the analysis of the Northridge earthquake. Their almost perfect agreement is promising for further research with the proposed methodology.

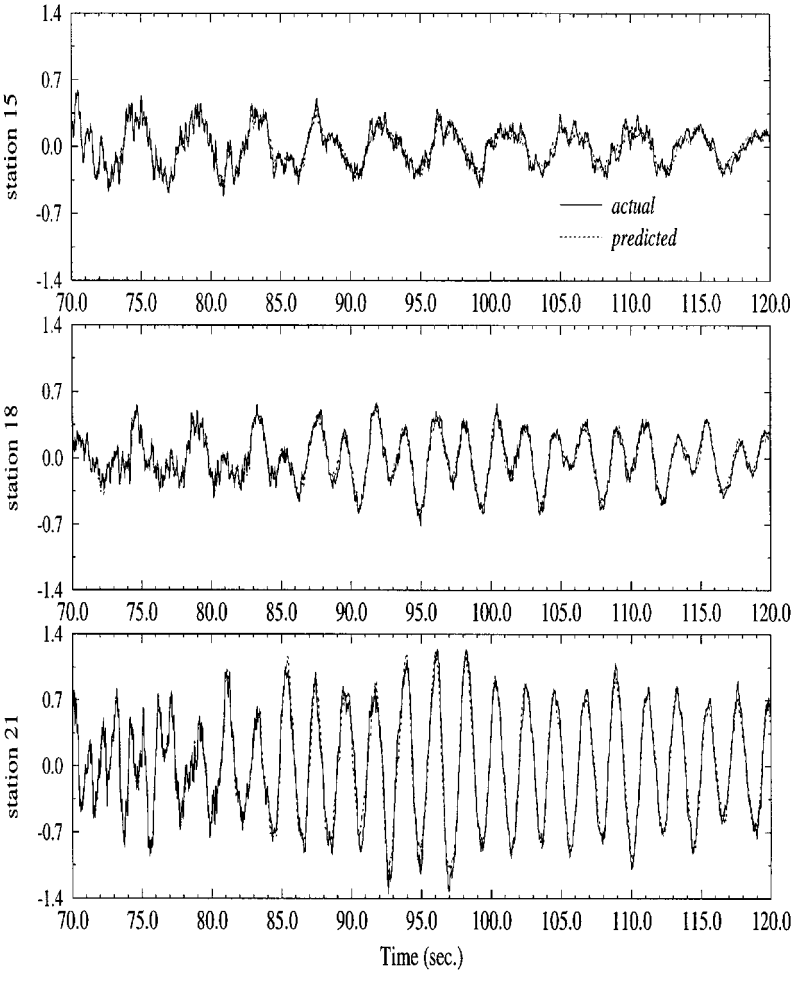

Figure 4. Actual and predicted accelerations (m/sec/sec) for the Vincent–Thomas Bridge during the Northridge earthquake

3.4. *Prediction of structural behaviour for future excitations*

Once the identification process has been completed, let us investigate how well the identified models can predict the structural response when the system is subjected to a previously unknown earthquake excitation.

For the 2-D model with four sensors, Figure 5 shows the time histories of the relative structural accelerations at four different levels (first, third, fifth and eighth floor, respectively) for the original system and for two identified models (corresponding to $p = 6$ and 17, identified with four output measurements) when they are subjected to an unknown 'future' earthquake. In this case, the seismic ground motion is represented by the El Centro earthquake 4s40e ground accelerations. Both identified systems show excellent agreement with the original system as confirmed in Figure 6, where the discrepancies between the original and the identified models are highlighted

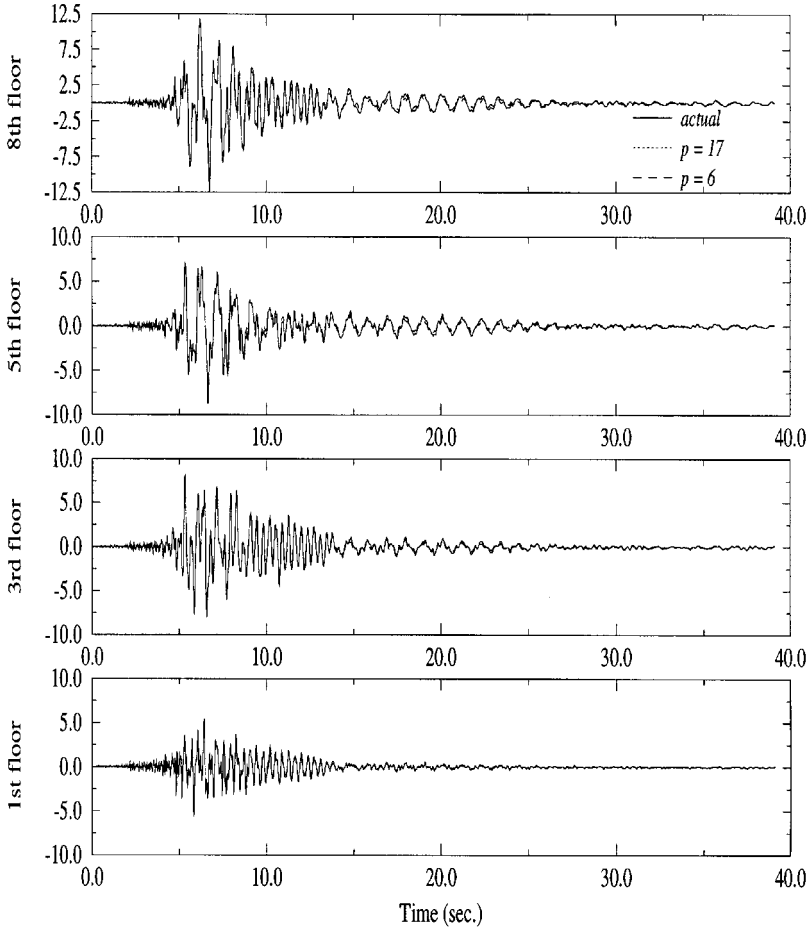

Figure 5. Response predictions (relative accelerations, m/sec/sec) of the actual and identified models (8-storey shear building with four sensors) subjected to El Centro 4s40e ground accelerations

more clearly. The visible part refers to the absolute errors in the predictions of the model identified with $p = 6$, while the absolute errors in the predictions using the model identified with $p = 17$ practically coincide with the zero axes.

For the 3-D model, the unknown 'future' ground excitation is represented by the time histories of the El Centro earthquake 4s40e and 4s50w ground accelerations acting simultaneously along the major and minor directions, respectively. For predicting the response, the model identified using only the relative accelerations of three joints on the eighth floor (two along the minor direction and one along the major direction) is used. This particular model was chosen because it showed a poor identification for the higher-order modes (see Table III). Figure 7 shows the time histories of the actual and the predicted relative accelerations on the eighth floor for the El Centro ground excitation and confirms that the predicted response of such an identified model is very close to the actual response (with the maximum relative error less than 10 per cent).

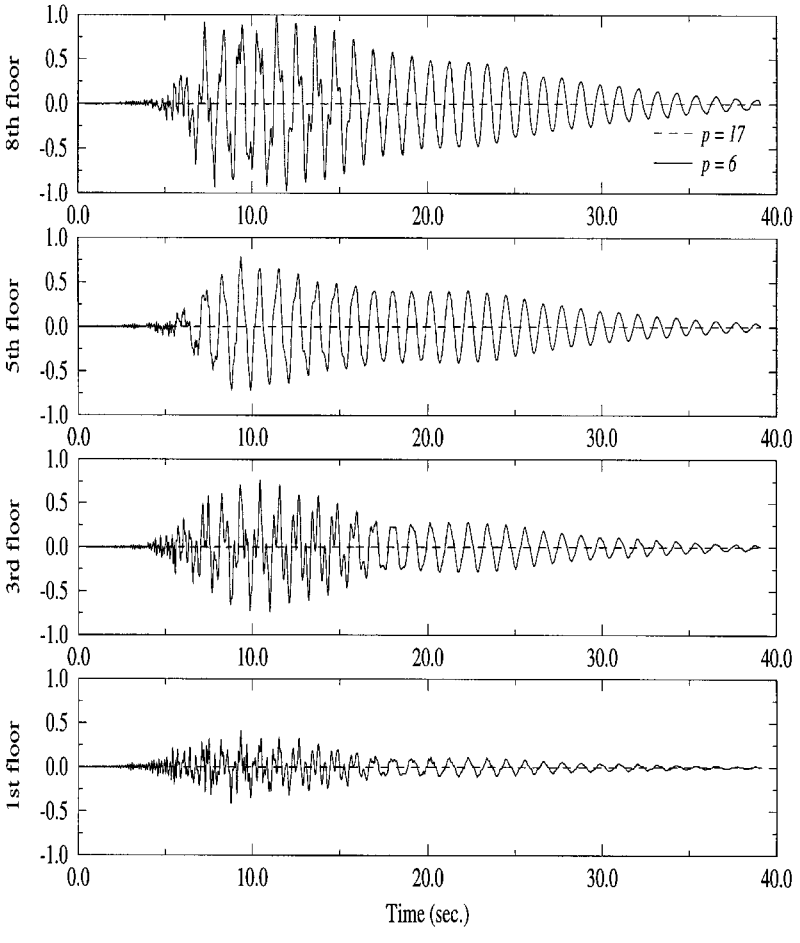

Figure 6. Absolute errors in response predictions (m/sec/sec) of the identified models (8-storey shear building with four sensors)

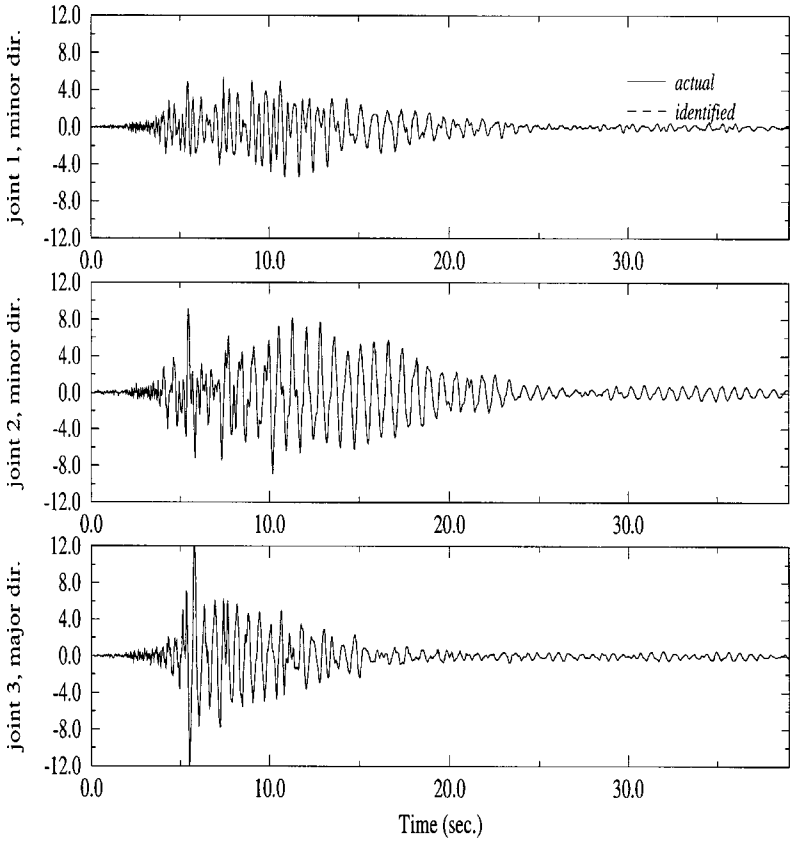

Figure 7. Response predictions (relative accelerations, m/sec/sec) of the three-dimensional actual and identified models subjected to El Centro 4s40e and 4s50w ground accelerations

3.5. Comparison with other S.I. methodologies

By comparing the results obtained using the proposed methodology with those from previous studies, it is possible to highlight the efficiency and accuracy of the OKID/ERA technique. Most experiments reported in the literature are either SISO systems[11,12,14,15] or 2-D structural systems (shear-type or chain-type) with a number of DOFs smaller than the examples considered in this study.[10,18] In addition, most of the model updating methods assume uncoupled modal damping.[7] On the contrary, the proposed OKID/ERA based identification technique has proven to be effective in determining state-space models of complex 3-D large MIMO structural systems, even with limited information and without any preprocessing of the data. No *a priori* assumption on the coupling of the second-order modes is necessary and the proposed technique has proven successful even in cases where modes are known to be coupled, e.g. the Vincent–Thomas cable suspension bridge.

In general, it is much more difficult to obtain an adequate input–output mapping and to predict structural behaviour for MIMO systems, especially for complex structures. The numerical

results discussed above clearly indicate that the proposed methodology is quite successful in properly addressing these issues. It should also be mentioned that during the studies performed on the Hubble space telescope, the OKID methodology reportedly produced extremely satisfactory results where most other approaches failed.[32]

4. CONCLUSIONS

In this paper, the authors have presented an efficient system identification algorithm for application to civil engineering structures. This algorithm is based on the Eigensystem Realization Algorithm and on the Observer/Kalman filter IDentification approach. The proposed methodology uses earthquake induced ground accelerations and structural vibrations as input–output data sets for identification purposes. It is shown that the results, from both simulated and recorded data, are promising, even in the presence of measurement noise and for the cases where the number of output measurements is less than the number of modes one wishes to identify.

The benefits of this method are twofold: (i) the proposed identification method identifies the modal characteristics, such as natural frequencies and modal damping percentages, very accurately with the use of an observer and (ii) the realized model mimics the behaviour of the original system very well when subjected to an unknown ground excitation. This leads to better predictions of the structural behaviour for future excitations, and thereby reduces the chance of structural failure by making the possibilities known beforehand. Since accurate results in experimental modal analysis generally require adequate excitation of all the modes to be identified, the proposed algorithm might reduce the costs for future applications.

ACKNOWLEDGEMENTS

The authors wish to thank Prof. M. Q. Phan of Princeton University for his suggestions and for his contribution to the computer program. They would also like to acknowledge Prof. A. S. Smyth of Columbia University for his contribution on the analysis of the recorded bridge data. This research study was sponsored by the National Science Foundation under research grant CMS-9457305.

REFERENCES

1. J. He and D. J. Ewins, 'Analytical Stiffness Matrix Correction Using Measured Vibration Modes', *Modal Anal.: Int. J. Anal. Exp. Modal Anal.* **1**(3), 9–14 (1986).
2. F. M. Hemez, 'Theoretical and experimental correlation between finite element models and modal tests in the context of large flexible space structures', *Ph.D. Dissertation*, Dept. of Aerospace Engineering Sciences, University of Colorado, Boulder, C.O., 1993.
3. S. W. Doebling, C. H. Farrar, M. B. Prime and D. W. Shevitz, 'Damage identification and health monitoring of structural and mechanical systems from changes in their vibration characteristics: a literature review', *Los Alamos National Laboratory Report LA-13070-MS*, 1996.
4. J. N. Juang and R. S. Pappa, 'A comparative overview of modal testing and system identification for control of structures', *Shock Vib. Dig.* **20**(5), 4–15 (1988).
5. J. E. Mottershead and M. I. Friswell, 'Model Updating in Structural Dynamics: A Survey', *J. Sound Vib.* **165**(2), 347–375 (1993).
6. D. J. Ewins, *Modal Testing: Theory and Practice*, Research Studies Press, Letchworth, 1984.
7. J. L. Beck and P. C. Jennings, 'Structural identification using linear models and earthquake records', *Earthquake Engng. Struct. Dyn.* **8**, 145–160 (1980).
8. G. H. McVerry, 'Structural identification in the frequency domain from earthquake records', *Earthquake Engng. Struct. Dyn.* **8**, 161–180 (1980).

9. J. P. Stewart and G. L. Fenves, 'System identification for evaluating soil-structure interaction effects in buildings from strong motion recordings', *Earthquake Engng. Struct. Dyn.* **27**, 869–885 (1998).
10. C. G. Koh and L. M. See, 'Identification and uncertainty estimation of structural parameters', *J. Engng. Mech.* **120**(6), 1219–1236 (1993).
11. R. Ghanem and M. Shinozuka, 'Structural-system identification. I: theory', *J. Engng Mech.* **121**(2), 255–264 (1995).
12. M. Shinozuka and R. Ghanem, 'Structural-system identification. II: experimental verification', *J. Engng. Mech.* **121**(2), 265–273 (1995).
13. M. Hoshiya and A. Sutoh, 'Kalman filter-finite element method in identification', *J. Engng. Mech.* **119**(2), 197–210 (1991).
14. E. Şafak, 'Adaptive modeling, identification, and control of dynamic structural systems. I: theory', *J. Engng. Mech.* **115**(11), 2386–2405 (1989).
15. E. Şafak, 'Adaptive modeling, identification, and control of dynamic structural systems. II: applications', *J. Engng. Mech.* **115**(11), 2406–2426 (1989).
16. S. F. Masri, R. K. Miller, A. F. Saud and T. K. Caughey, 'Identification of nonlinear vibrating structures; Part I: formulation', *J. Appl. Mech. Trans. ASME*, **109**, 918–922 (1987).
17. S. F. Masri, R. K. Miller, A. F. Saud and T. K. Caughey, 'Identification of nonlinear vibrating structures; Part I: applications', *J. Appl. Mech. Trans. ASME*, **109**, 923–929 (1987).
18. C. C. Lin, T. T. Soong and H. G. Natke, 'Real-time system identification of degrading structures', *J. Engng. Mech.* **116**(10), 2258–2274 (1990).
19. H. G. Natke, 'Recent trends in system identification', in W. B. Kratzig *et al.* (eds), *Struct. Dynamics*, A. A. Balkema, Netherlands, 1991, pp. 283–289.
20. F. E. Udwadia, 'Methodology for optimum sensor locations for parameter identification in dynamic systems', *J. Engng. Mech.* **120**(2), 368–390 (1994).
21. J. L. Beck and L. S. Katafygiotis, 'Updating models and their uncertainties. I: Bayesian statistical framework', *J. Engng. Mech.* **124**(4), 455–461 (1998).
22. J. L. Beck and L. S. Katafygiotis, 'Updating models and their uncertainties. II: Model identifiability', *J. Engng. Mech.* **124**(4), 463–467 (1998).
23. A. W. Smyth, S. F. Masri, A. G. Chassiakos and T. K. Caughey, 'On-line parametric identification of MDOF nonlinear hysteretic systems', *J. Engng. Mech.* **125**(2), 133–142 (1999).
24. E. G. Gilbert, 'Controllability and observability in multivariable control systems', *SIAM J. Control* **1**(2), 128–151 (1963).
25. R. E. Kalman, 'Mathematical description of linear dynamical systems', *SIAM J. Control* **1**(2), 152–192 (1963).
26. J. N. Juang and R. S. Pappa, 'An eigensystem realization algorithm for model parameter identification and model reduction', *J. Guidance Control Dyn.* **8**(5), 620–627 (1985).
27. B. L. Ho and R. E. Kalman, 'Effective construction of linear state-variable models from input/output functions', *Proc. 3rd Allerton Conf. Circuit and Systems Theory*, pp. 449–459, 1965.
28. L. M. Silverman, 'Realization of linear dynamical systems', *IEEE Trans. Automat. Control* **AC-16**(6), 554–567 (1971).
29. M. Phan, J. N. Juang and R. W. Longman, 'On Markov parameters in system identification', *NASA Technical Memorandum* 104156, 1991.
30. J. N. Juang, J. E. Cooper and J. R. Wright, 'An eigensystem realization algorithm using data correlations (ERA/DC) for model parameter identification', *Control Theory Adv. Technol.* **4**(1), 5–14 (1988).
31. M. Phan, L. G. Horta, J. N. Juang and R. W. Longman, 'Linear system identification via an asymptotically stable observer', *J. Optim. Theory Appl.* **79**(1), 59–86 (1993).
32. J. N. Juang, M. Phan, L. G. Horta and R. W. Longman, 'Identification of observer/Kalman filter Markov parameters: theory and experiments', *J. Guidance Control Dyn.* **16**(2), 320–329 (1993).
33. J. N. Yang, A. Akbarpour and P. Ghaemmaghami, 'New optimal control algorithms for structural control', *J. Engng. Mech.* **113**(9), 1369–1386 (1987).
34. D.-H. Tseng, R. W. Longman and J. N. Juang, 'Identification of gyroscopic and nongyroscopic second order mechnical systems including repeated problems', *Adv. Astronaut. Sci.* **87**, 145–165 (1994).
35. D.-H. Tseng, R. W. Longman and J. N. Juang, 'Identification of the structure of the damping matrix in second order mechanical systems', *Adv. Astronaut. Sci.* **87**, 166–190 (1994).
36. A. M. Niazy, 'Seismic performance evaluation of suspension bridges', *Ph.D. Dissertation*, University of Southern California, 1991.

